Iraqi Journal for Computer Science and Mathematics

Manuscript 1247

An Improvement Finger Vein Authentication System Based on PCANet Deep Learning and Hyper Parameter Machine Learning

Raniah Ali Mustafa

Tarek Abbes

ORIGINAL STUDY

An Improvement Finger Vein Authentication System Based on PCANet Deep Learning and Hyper Parameter Machine Learning

Raniah Ali Mustafa *, Tarek Abbes

Innov'COM, National School of Electronics and Telecommunications of Sfax, University of Sfax, Tunisia

ABSTRACT

Finger vein authentication is a biometric technique that uses unique vein patterns within the finger to verify identity, ensuring security by scanning veins with near-infrared light to prevent counterfeiting. The reliability of this technology and its resistance to skin disorders make it highly appreciated. The motivation for using PCANet deep learning in finger vein authentication arises from the need for a more precise, secure, and effective biometric system. Conventional methods have trouble with image quality, noise, and illumination, whereas PCANet improves classification accuracy by employing principal component analysis (PCA) to extract deep features. Its lightweight structure guarantees computational efficiency while maintaining a high level of security, making it ideal for applications that require robust authentication. By using high-quality data and lowering the computational complexity needed by the PCANet approach, the suggested system seeks to increase performance. This research introduces three approaches: high-frequency emphasis filtering (HFEF), gabor filter (GF) images, and novel enhanced image techniques using contrast-limited adaptive histogram equalization (CLAHE) to keep edges and increase image quality. Second, for dimensionality reduction and feature extraction, a novel integrated PCANet as well as feature-level principal component analysis (PCA) is suggested. Ultimately, a pair of authentication models are chosen: one employing hyperparameter machine learning (HPML) in conjunction with Multi-Layer Perceptron (MLP), K-Nearest Neighbors (KNN), and Support Vector Machine (SVM) for random search, and the other using the same techniques for simple search. PLUSVein-Contactless finger vein dataset was used for evaluating such techniques. The suggested approaches performed better on this dataset, with an F1 score of some metrics of 100% for SVM, 99.90% for KNN, and 100% for MLP. Those results were for the random search model with PCA. The outcomes demonstrated a considerable improvement in F1-score of finger vein authentication using PCANet DL, both without and with PCA. Furthermore, the suggested authentication mechanism outperformed previously suggested approaches, in terms of improved image quality, good vein-specific features, and obtaining the best set of optimal parameters for matching.

Keywords: Finger vein authentication, Hyperparameters machine learning, Model parameter machine learning, PCANet deep learning

1. Introduction

Recently, the biometrics field has increasingly focused on finger-vein authentication, drawn by its unique advantages over more traditional biometric identifiers such as fingerprints, iris scans, palm print analysis, and facial recognition [1]. A finger vein authentication system secures identity by analyzing unique, unalterable vein patterns under the skin, offering robust biometric security. Unlike fingerprints, veins cannot be stolen or counterfeited, and contactless nature reduces the risk of disease transmission. Finger vein patterns remain stable throughout life, eliminating the need for re-registration [2]. Due to

Received 12 October 2024; revised 25 February 2025; accepted 9 March 2025.
Available online 26 April 2025

* Corresponding author.
E-mail addresses: rania83computer@uomustansiriyah.edu.iq (R. A. Mustafa), tarek.abbes@enetcom.usf.tn (T. Abbes).

https://doi.org/10.52866/2788-7421.1247

hygiene considerations, contactless biometrics such as finger veins are expected to be most beneficial in the future. Finger vein biometrics have multiple uses. Finger vein biometric authentication lets users "access networks" (AN), "web apps" (WA), "web portals" (WP), and other resources without remembering complex passwords. Credit card authentication and online transactions can be used in banking to enhance client security and convenience [3]. Finger vein authentication speeds up login, eliminates the need for passwords, and reduces reset costs. It's used for physical access control in airports, security systems, and more, minimizing issues with lost or stolen cards and keys. Infrared or visible light scanners detect hemoglobin in veins, enabling registration and authentication [4]. Machine learning (ML) techniques have been employed for authentication by numerous biometrics researchers [5, 6]. In order to develop a format appropriate for classification, unprocessed biometric data must have its features extracted using extraction methods in order for ML algorithms to function. Moreover, before moving further with feature extraction (FE), certain preprocessing operations on ML algorithms must be completed. Furthermore, it must be mentioned that certain extraction techniques could not always produce the desired results when used with different biometric kinds or different datasets which pertain to the same biometric. Furthermore, they cannot manage biometric image changes, like rotation and zooming [7, 8]. Deep learning (DL) has emerged as a significant, influential factor in biometric systems, yielding remarkable outcomes [9, 10]. DL algorithms effectively address the shortcomings of traditional ML algorithms, particularly those related to feature extraction approaches. Advanced DL algorithms can extract features from raw data and handle biometric image alterations [11].

Although previous research has examined vein identification, authentication systems still face challenges in extracting finger vein features and improving image quality. Few studies have concentrated on enhancing vein texture and contrast during feature extraction (FE) and image enhancement. The main problems related to finger vein image enhancement and FE that this research aims to address include: (a) low contrast and poor quality of vein-specific features in finger vein images, leading to problems like improving contrast, overemphasizing bright areas, and underemphasizing dark ones. (b) Many current enhancement methods only address contrast improvement, but a single filter strategy is often inadequate. (c) The use of numerous complex feature extraction methods in finger vein systems limits their practicality in real-world applications. Given the limitations of previous studies, this research seeks to address problems such as poor image quality, laborious classification, and high computational costs.

Research on hyperparameter machine learning (HPML) for finger vein authentication has not yet been done, as far as we are aware. It was challenging to identify the ideal characteristics that result in a high identification rate. To identify the best approach, pre-processing techniques were first applied. After experimenting with a number of techniques, PCANet approach was chosen in the end to extract features using PCA. After utilizing a variety of classification techniques, we ultimately determined that the SVM, KNN, and MLP fit the PCANet approach with PCA the best. Additionally, it is noted that we have used the PLUSVein-Contactless dataset to test our approaches. More particular, our research makes the following contributions:

- Development regarding a finger vein enhancement method which combines three methods (CLAHE, GF, and HFEF) to eliminate noise, improve contrast, and emphasize the veins' texture.
- Proposed a fusion feature extraction method to derive structure features (middle, index, and ring) from finger vein images of the two hands. Additionally, extract features for the middle, index, and ring fingers separately to obtain individual fusion for each hand.
- Combined PCANet deep learning and feature-level PCA to enhance system performance through feature extraction and dimensionality reduction.
- Utilized two machine models: a simple search with MPML and a random search with HPML to improve the authentication system.

The remainder of this research is organized as follows: the related works are reviewed in Section 2. The procedures are explained in Section 3. The evaluation findings for each approach are shown in Section 4. The comparison and discussion are given in Section 5. The conclusion is discussed in Section 6.

2. Related works

The limitations and efficiency of different finger vein feature extraction as well as recognition techniques will be thoroughly reviewed and analyzed in this section's extensive examination of recent literature. A new method that makes use of the weighted Local Binary Pattern (LBP) method was presented by Lee et al. [12]. Initially, vein pattern detection has been omitted in favor of extracting holistic codes using the LBP approach, which greatly reduced processing time. Local vein pattern areas are then divided into three separate groups using such LBP codes and a SVM classifier [13, 14]. The classification regarding such local areas determines the different weights that are allocated to the LBP codes. With finger vein analysis based solely on texture information, the classification result will be less accurate. Linear discriminant analysis (LDA) and Principle component analysis (PCA) have been utilized by Liu and Wu [15] for FE as well as dimensionality reduction throughout image preprocessing. SVM [13, 14] were used in conjunction with adaptive Neuro-fuzzy inference system (ANFIS) for classification. However, there are a lot of heuristics in fuzzy methodology. The number of subjects in the data-set is limited, and classification process takes a very lengthy time. Khellat-Kihel et al. [16] used an SVM classifier for classifying features derived by applying Gabor Filter (GF) [17] on the PKU (V2) dataset for improving finger vein images with the use of CLAHE [18, 19]. The inefficiency of feature extraction techniques led to low SVM classification accuracy for finger veins. A novel technique depending on Gradient Boosted (GB) feature extraction algorithm was presented by Ganesan and Kalaimathi [20] to assess the SVM [13, 14] approach for classifying finger vein images. Mukahar, Han, and Rosdi [21] develop a new finger vein image classification system. On Finger Vein USM (FV-USM) dataset [22], experiments have been carried out with the use of adaptive k-nearest centroid neighbour (akNCN) which improved the kNCN classifier for extracting features with the use of PCA algorithm. The inability to identify the appropriate number of neighbor sizes throughout the classification stage resulted in a decrease in the akNCN's accuracy in classifying finger veins. Back-propagation (BP) network as well as integrated adaptive Neuro-Fuzzy Inference System (ANFIS) are used in Wu and Liu's [23] suggested finger vein authentication technique. PCA is used as the feature extraction approach. Ten samples per finger and ten subjects in total. The system exhibited high accuracy even with limited training of the feature vector, yet the classification times were also long. In order to identify the individual and extract low-dimensional information from finger vein images using the PCA approach, He et al. [24] used a BP network. A total of 600 images were processed using the recommended procedure. BP network's non-linear classification took a long time to train, and the accuracy is still not up to par. Through identifying finger vein patterns with the use of a proposed Neuro-fuzzy as well as BP network and extracting the optimal features utilizing Genetic PCA method, R and David [25] have demonstrated that the authentication systems have good accuracy. One hundred and fifty image samples from the "SDUMLA-HMT" dataset [26] were used in the tests. The findings demonstrated that the optimization features of GPCA and PCA were inaccurate since they did not offer a more thorough parameter analysis and only included a limited number of images. FVRS, or Finger Vein Recognition System, was suggested by Wen et al. [27]. Feature extraction was carried out using the Principal Component Analysis Network (PCANet) technique. For the classifier FVRS, KNN with Euclidean distance (ED) has been used. The identification time is highly influenced by KNN's k-value. The significance of this parameter in KNN method is highlighted by the fact that as k-value increases, so does the identification time. Furthermore, a reduced number of visible finger veins on the subject also meant a longer time. Khanam et al. [28] introduced the KNN and discriminant analysis (DA) algorithms to assess and calculate the accuracy of the feature extracted from images of finger veins. With "Fast Retina Key Point" (FRKP) descriptors, features were extracted with the use of "features Accelerated Segment Test" (FAST) method. The minimum recognition rate in the KNN algorithm is because the image quality is not good even after all suggested pretreatment stages, utilizing a public dataset of finger veins called "SDUMLA-HMT." Shazeeda et al. [29] used the KNN algorithm in conjunction with a sparse representation-based classifier (SRC) to develop a novel method for individual identification depending on finger vein images. This method is known as (KNN-SRC). According to an analysis regarding the experimental results on FV-USM data-base [22], this method is computationally demanding, particularly when the number of samples being trained grows and the accuracy might be severely affected by features that are noisy or irrelevant. In order to decrease hidden nodes and enhance the functionality of the finger vein system, Xie et al. [30] have introduced feature component-based Extreme Learning Machines (FC-ELMs). However, the input-hidden layer of the extreme learning machine has arbitrary weights, which results in unstable performance until weight optimization is accomplished. Padmapriya et al. [31] presented an authentication system that relied on finger veins. Convolutional Neural Networks (CNN) are used to extract features and match finger vein images to classify authentic or fake. The dataset used in the authentication system is collected by placing the finger in the correct position and capturing it using a charge-coupled device (CCD) camera. Although the authentication system achieved good results, it suffered from the quality of the finger vein images due to insufficient illumination and problems in the scanner device which led to inexact results in the authentication system. An efficient system for finger vein authentication was designed by Rehman et al. [32], Using scattering wavelet (SW) which is similar to the CNN approach to extract features from finger vein images. For matching, employ two methods KNN and SVM for machine learning. Using the SDUMLA-HMT, and FV-USM datasets, the system achieved a good result. The methods used for extracting features require high quality for finger veins, due to poor quality images, which results in an authentication system, which is considered a challenge in the biometric system. Prommegger et al. [33] introduced a CNN-based approach for finger veins. Uses three networks (Mask R-CNN, CCNet and HRNet) for segmentation which are implemented on (HKPU, PLUSVein-Contactless finger vein, PMMDB, and UTFVP) datasets. The suggested approach achieved good results for segmentation. CNNs have benefits over classical approaches but need more computational resources and are difficult to implement. A limited number of samples in a training set, poor image quality, laborious classification, and high computational costs are among the most common drawbacks of the majority of review systems in use today. The high-performance authentication method proposed in this study aims to overcome such limitations and perhaps advance the field.

3. Research methods and material

The purpose of this section is to describe the suggested approaches and dataset for the finger vein authentication system. PCANet network's DL phases are covered in this study.

3.1. Description of the dataset

The contactless acquisition of such datasets creates various finger/hand misplacements in data (bending, tilts, non-planar rotations and in-planar), making finger/hand normalization difficult. It has 42 individuals, two hands (right and left), six fingers (right and left index, ring, and middle finger), and five images per finger/hand were taken during a single session for each subset. A palmar finger subset and a palmar hand vein subset make up its two subsets. Thus, there are 252 distinct fingers in the finger vein subset and 84 distinct hands in the hand vein subset. Consequently, there are 1260 images in subset of images for the finger vein and 840 images in total (two illumination adjustments, 850 nm and 950nm, 420images each) in the subset of images for the hand vein. There are two hundred and one images in the data-set. The raw images with a resolution of 1280 × 1024 are stored in the 8-bit greyscale PNG format [4, 34]. The motivation for adopting the finger vein dataset in our framework is that there are six fingers (index, ring, and middle finger) on both hands of the same individual. Since we suggested a novel technique to enhance image quality used in our research work, it will lead to an increase in the dataset as there will be a greater quantity of images. This technique will increase to five new images for every original image in the subset, making a total of 7,560 images to be utilized in the system. For testing and training, the dataset was divided into 30% and 70%, respectively.

3.2. PCANet deep learning

PCANet is a simple DL network that is frequently utilized for feature extraction (FE) in image classification. Compared to other DL networks, such the convolution deep NN (ConvNet), PCANet takes less training effort. PCANet uses three basic processing components [35, 36].

(1) Use PCA Filter Banks to extract high-level features through cascaded PCA.
(2) Binary hashing (BH).
(3) Histograms (Hist).

The steps of PCANet are as follows:

PCA filter bank: There are two filter bank convolution stages in the PCA filter bank. Using the PCA approach on the filters, the first step entails estimating the filter banks. Every vector within the filter set denotes a k1 × k2 narrow window around a single point (pixel) of a certain feature, such a finger vein. The average of each vector element is then subtracted from the average of all vector elements, which has been calculated. The principal components (W of size $k_1 \times k_2 \times L_{S1}$) are then preserved by performing PCA on these vectors, with L_{S1} serving as the basis eigenvector. On the other hand, every principal component W is regarded as a filter and is convertible to a $k_1 \times k_2$ kernel. The input image was combined using this filter in the following manner:

$$I_1(x, y) = h_1(x, y) * I(x, y), \quad (1)$$

In which * indicates discrete convolution. $I \in [1.1_{s_1}]$. I is the final image that has been filtered with the h filter.

PCANet's second stage is executed out by repeating the algorithm for each of the first stage's output images. The procedure involves considering the mean for each output image I. After that, the average was removed from each vector-computed input. Then, a second vector and another PCA filter bank (using L_{S2} filters) are estimated by concatenating each vector. Finally, every acquired filter is combined with I to generate a new image.

$$I_{1,m}(x, y) = h_m(x, y) * I_1(x, y), \quad (2)$$

Consequently, with the use of output images from first stage, repeat the convolution step for the two filters, L_{S1} and L_{S2}, for obtaining output images.

Binary Hashing (BH): This part involves the conversion of the output L_{S1} and L_{S2}, which were obtained in the previous stage, to binary data with the use of Heaviside step function, which is:

$$I_{1,m}B(i,j) = \begin{cases} 1 & if \quad I_{1,m}(i,j) \geq 0 \\ 0 & otherwise \end{cases} \tag{3}$$

Where $I^{B}_{1,m}$ The binary bit vector L_{S2} is then obtained as a decimal number around each pixel. Thus, in this work, a single integer value (image) is produced from the L_{S2} output.

$$I^{D}_{I}(i,j) = \sum_{m=1}^{L_{s2}} 2^{m-1} I^{B}_{I,m}(i,j) \tag{4}$$

Where I^{D}_{I} indicates the hashed image. Every pixel value is an integer in the range $[0, 2^{L_{s2-1}}]$.

Histograms (Hist): Every hashed image I^{D}_{1} is divided into NB blocks in this last stage. Next, each block's (B) histogram is calculated. Keep in mind that depending on the application or disjoint, these blocks may be non-overlapping or overlapping, respectively. Consequently, all of the blocks' histograms B are associated in the following way to obtain the characteristics that were derived from I^{D}_{1}:

$$V^{hist}_{1} = \left[B^{hist}_{1}, B^{hist}_{2}, B^{hist}_{NB}\right] \tag{5}$$

Following the encoding phase, the input image I feature vector is concatenated:

$$V^{hist}_{1} = \left[V^{hist}_{1}, V^{hist}_{2}, V^{hist}_{L_{s1}}\right] \tag{6}$$

3.3. Proposed method

Fig. 1 shows the general architecture regarding the finger vein authentication system. The procedure is divided into three primary phases: matching, preprocessing, and feature extraction. Every stage is made up of multiple steps that are used to identify each test sample and establish if they are all from the same individual.

3.3.1. Preprocessing stage

The initial step in getting input images ready for subsequent steps is called preprocessing. It seeks to improve a low-contrast image by raising its quality and sharpness, making it easier to extract features. At this point, the suggested enhanced approach, which uses three techniques, improves the finger vein image: The Gabor Filter (GF) is used in the first approach [17], CLAHE is used in the second approach [18, 19], histogram equalization (HE) is followed by median filter filtering [37], and Fourier Transform (FT) is used in the final approach [38] for high-frequency emphasis filtering. In this work, we used the discrete cosine transform (DCT) approach to integrate three images that were generated using three different approaches (CLAHE, GF, and HFEF). After the final image has undergone contrast adjustment, the final image is referred to as the image fusion. Below are the specifics of each stage in the suggested approach.

- **Proposed Image Fusion**

Image fusion combines all relevant information from each image to produce a single image from many images. Discrete Cosine Transform (DCT)-depend approaches for image fusion are highly efficient and time-saving in real-time systems which use DCT-depend standards for still images. 2D DCT transform method used in this study could be used to obtain x (m, n), which is the value of a NxN block in the image [38].

$$d(k,I) = \frac{2\alpha(k)\alpha(1)}{N} \cdot \sum_{m=0}^{N-1}\sum_{n=0}^{N-1} x(m,n) \cdot \cos\left(\frac{(2m+1)\pi k}{2N}\right) \cdot \cos\left(\frac{(2n+1)\pi k}{2N}\right) \tag{7}$$

Where in $k, 1 = 0, 1, \ldots, N-1$ and

$$\alpha(k) = \begin{cases} \frac{1}{\sqrt{2}} & if \quad k = 0 \\ 1 & otherwise \end{cases} \tag{8}$$

Inverse DCT transform (IDCT) could be obtained using the equations [38].

$$x(m,n) = \sum_{k=0}^{N-1}\sum_{I=0}^{N-1} \frac{2\alpha(k)\alpha(1)}{N} \cdot d(k,1) \cdot \cos\left(\frac{(2m+1)\pi k}{2N}\right) \cdot \cos\left(\frac{(2n+1)\pi k}{2N}\right) \tag{9}$$

Where $m, n = 0, 1, \ldots, N-1$.

In Eq. (3), d (0,0) denotes to DC coefficients, whereas d (k, l) is AC coefficient in the block, and could be acquired with the use of the equation:

$$\hat{d}(k,I) = \frac{d(k,I)}{N} \tag{10}$$

The average value (AV), μ and variance, α^2, for N × N block through spatial domain (SD) can be obtained using the equations:

$$\mu = \frac{1}{N^2}\sum_{m=0}^{N-1}\sum_{n=0}^{N-1} x(m,n) \tag{11}$$

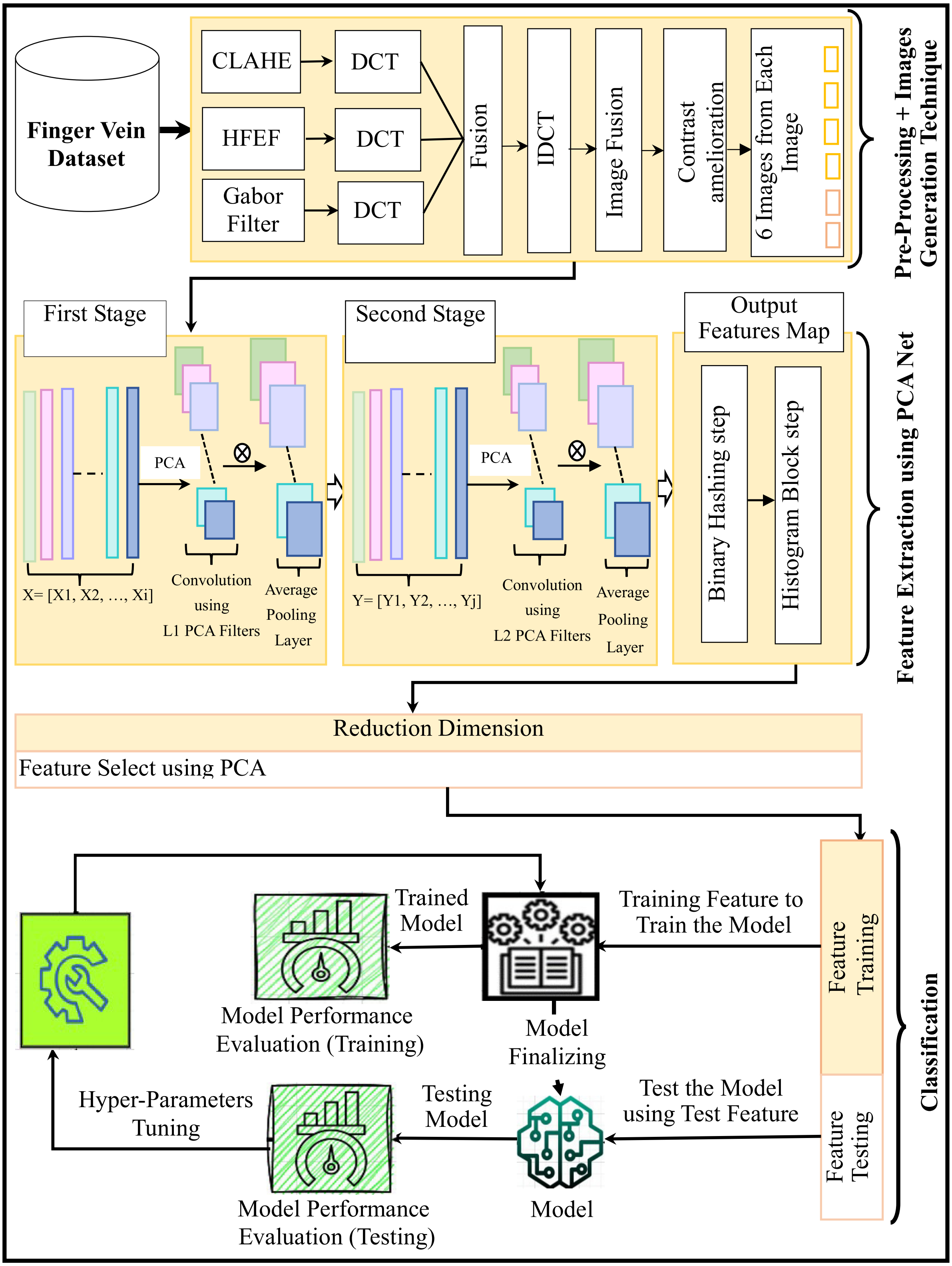

Fig. 1. Proposed framework.

Algorithm 1. The Proposed Image Fusion

Input: Original Finger Vein Image
Output: Image Fusion
BEGIN
Step1: Read the original Finger Vein image
Step2: FOR each row (I) from 1 to image height:450pixels
Step3: FOR each column (J) from 1 to image width:150pixels
Step4: Split the image into an 8 × 8 block
Step5: **Preprocessing Steps**
Step5-1: Apply Gabor Filter
Step5-2: Apply Contrast Limited Adaptive Histogram Equalization (CLAHE)
Step5-3: Apply High-Frequency Emphasis Filtering (HFEF) with Fourier Transform (FT)
Step6: **Feature Extraction**
Compute the Discrete Cosine Transform (DCT) for each of the processed images (GF, CLAHE, HFEF)
Step7: **Variance Calculation**
Compute the variance for each of the processed images (GF, CLAHE, HFEF)
Step8: **Block Selection**
Select the block with highest value of variance, and eliminate the other block
Step9: **Fusion Method**
Create a DCT fusion method by combining coefficients from the selected block
Step10: **Inverse Transform**
Compute the Inverse DCT transform (IDCT) to obtain the fused image in spatial domain
Step11: **Contrast Enhancement**
Apply contrast amelioration to enhance the final fused image
Step12: **END FOR (J)**
Step13: **END FOR (I)**
Step14: return Final Result
Step15: **END**

$$\alpha^2 = \frac{1}{N^2} \sum_{m=0}^{N-1} \sum_{n=0}^{N-1} x(m, n) - \mu^2 \tag{12}$$

DCT coefficients of N × N block of pixels are used to calculate the variance in the block. The following equation could be used to determine them once the normalized and squared AC coefficients have been added to the DCT block:

$$\alpha^2 = \sum_{k=0}^{N-1} \sum_{I=0}^{N-1} \frac{d^2(k, I)}{N^2} - d^2(0, 0) \tag{13}$$

In applications involving image processing, the variance value is interpreted as a measure of contrast. In addition to that, the fusion method, which employs DCT, has been built around maximum information that is available for each one of the pixel blocks for the two DCT images. The data that has been utilized in this instance was derived from the variance values of each block [39]. DCT fusion approach's main premise is to identify the block with the most information. Therefore, HE and Gabor Filtering (GF) blocks of the two images were compared in this study. After selecting the block with the highest variance value, the other has been disregarded. From both processed DCT images, a final DCT image could be produced by applying the following equation:

$$d_{fus}(i, j) = \begin{cases} d_{HE}(i, j) & if \ \text{var}_{d_{HE}} > \text{var}_{d_{GF}} \\ d_{GF}(i, j) & if \ \text{var}_{d_{HE}} < \text{var}_{d_{GF}} \\ d_{HF}(i, j) & if \ \text{var}_{d_{HE}} < \text{var}_{d_{HF}} \end{cases} \tag{14}$$

Algo. 1 summarizes the proposed image enhancement method.

Examples of the outputs of three image enhancement methods as well as the proposed image fusion method and contrast-enhanced method with histogram for some finger vein samples are presented in Fig. 2. As a result of the preprocessing stage, five images were obtained from each original image of a single finger, to generate a total of 6 images (Original, Gabor, CLAHE, HFEF, Image Fusion, and Contrast Image Fusion), which were later used in the training process.

3.3.2. Feature extraction stage

For obtaining a 1-D feature vector for each finger vein, we concentrate on using each PCANet as a

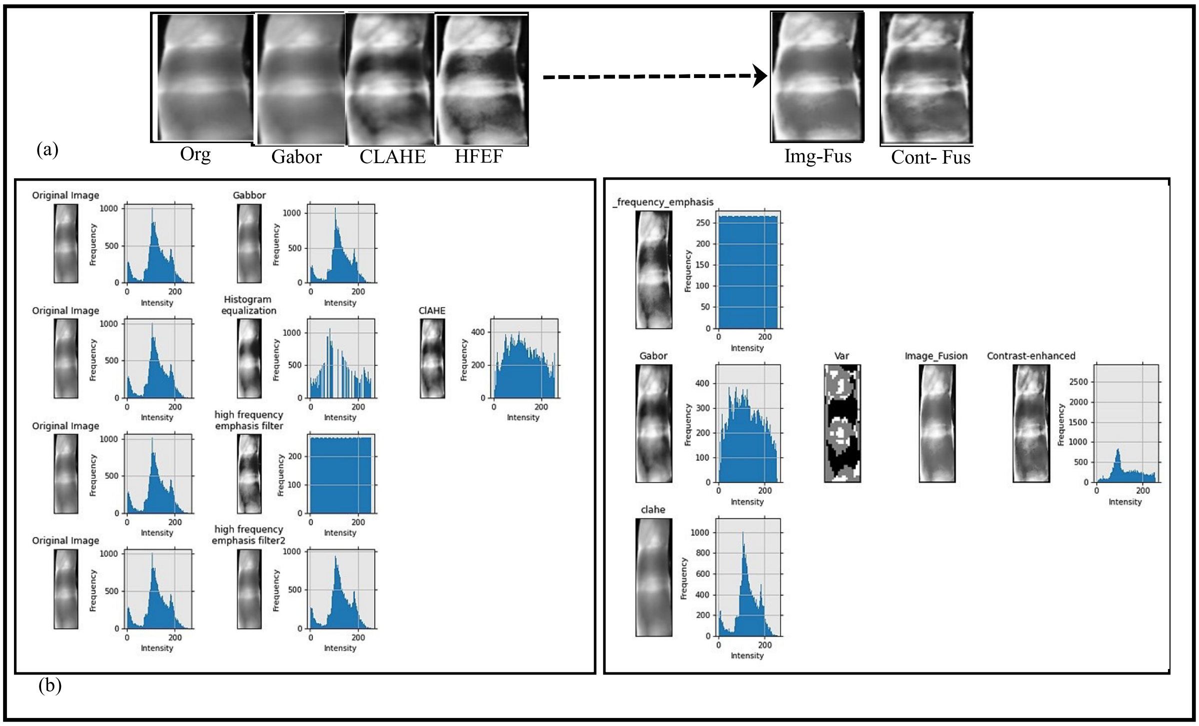

Fig. 2. Show enhanced images (a) Result of some samples of finger vein images (Original, Gabor, CLAHE, HFEF, image fusion, and contrast image fusion) (b) Results images with histogram.

Table 1. PCA net parameters for finger vein.

Finger Vein				
No. of Stages	No. of Filters	Filter Size	Block Size	Overlapping
2	[7 7]	[4 4]	[21 21]	0.5%

model which incorporates PCA into the corresponding DL model on the corresponding vein data. These large, highly dimensional vectors undergo dimensionality reduction prior to the matching stage. One popular and easy technique for lowering dimensionality is PCA [40, 41]. In this work, the key features were extracted using PCANet before anything else. Their parameters ought to be established by this effort. The number of stages (Ns), the number of filters in every stage (Lsi), the block size for local histograms in output layer, and the filter size (k1; k2) are among the PCANet parameters. Setting these initializations is required in order to assess the performance of the recently proposed PCANet-based approach. In order to create the best features that accurately describe input finger vein properties, such factors are crucial. Improving the authentication system's performance is also intriguing. These experimentally determined characteristics are displayed in Table 1.

Example of the results produced by PCANet. The image below displays the four filter results from the PCANet layer and the outputs for PCANet following the hashing phase, as illustrated in Fig. 3.

In the presented study, we concentrate on dimensionality reduction and feature extraction from images of the index, middle, and ring veins in both hands. In order to improve the authentication system, we suggested feature-level fusion, which combines different features from different finger veins. After obtaining three distinct feature fusions, we examined the suggested approach's authentication accuracy using the fusion step that was outlined in the matching stage. For the position of finger vein areas in the context of finger-based biometric authentication, the results for the suggested feature-level fusion are shown in Fig. 4.

From the results of feature vectors, compatibility between numerous feature vectors (FVs) from various types of feature-level fusion can be used to create high-dimensional feature vectors (FVs). In the way, for each class, we have indicated 180 right and left finger vein images of both hands were trained by PCANet feature-level with and without PCA dimensionality reduction to obtain the best feature vectors (FVs), where the one dimensions of the feature vector are (1×768). Integrating feature-level information is difficult due feature sets from different biometric modalities may not be compatible or accessible.

3.3.3. Hyper parameters tuning stage

To obtain shift matrices of the finger vein, the matching stage of the newly proposed system relies

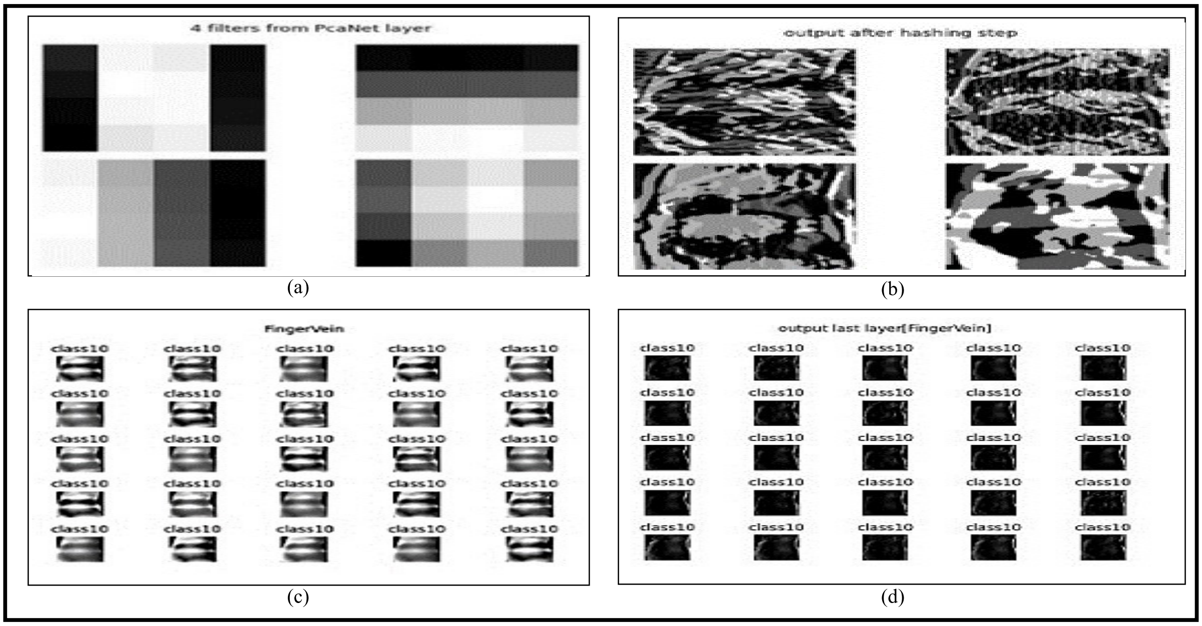

Fig. 3. Visual result of PCA net workflow (a) Filters from PCA net layer (b) Output after first hashing step (c) Output of the some samples for finger vein after hashing steps (d) Output of last layer.

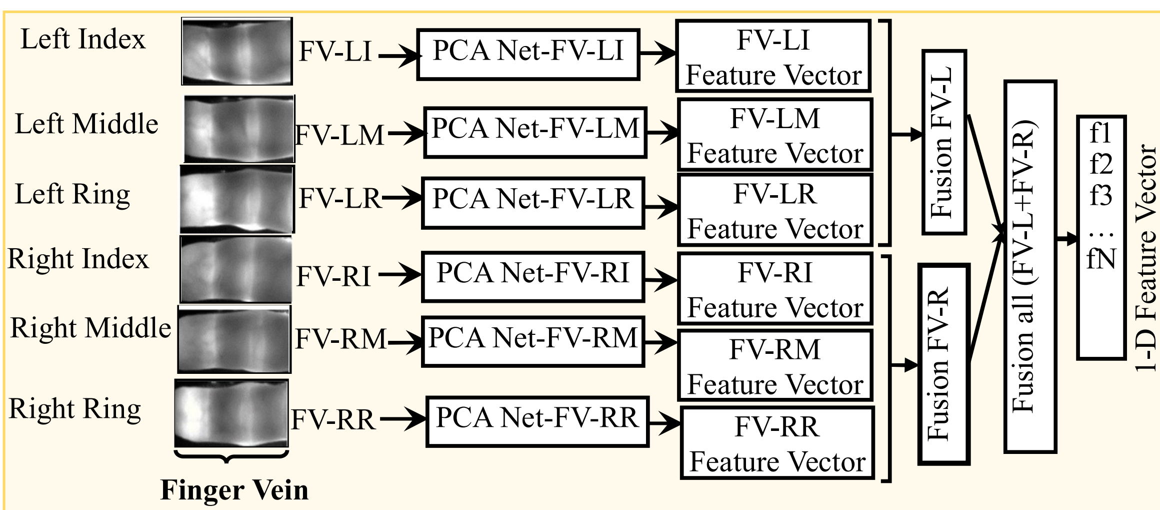

Fig. 4. Outline proposed feature-level fusion for finger vein position.

on the authentication models. HyperParameter (HPML) and Model Parameter (MPML) are the two categories of ML model parameters.

Simple search model (MPML): These are the model parameters that are required to be implemented using the training set, which corresponds to the fitted parameters.

Random search model (HPML): These are modification parameters that require modification to obtain the optimum set of parameters for model performance.

In the presented study, we developed techniques (KNN [42], MLP [43], and SVM [13, 14]) to determine the optimal hyperparameter set using the Model Parameter and the HyperParameter tuning model. We divided the dataset in the working framework into two sets: 2,268 finger vein data samples were utilized for testing, and 5,292 finger vein data samples were utilized for the training. The model is trained on the training set of data with the use of MLP, KNN, and SVM algorithms for assessing the model's performance. The performance of the model is evaluated after that by testing it with the test data. Our suggestion was a hyperparameter tweaking model to improve the authentication system's effectiveness. We determined the ideal parameters

Table 2. Optimal parameters for random search model (HPML) for some samples.

	HPML (KNN)	HPML (MLP)	HPML (SVM)
Fusion-all-FV	{'weights': 'uniform', 'p': 1, 'n_neighbors': 1, 'algorithm': 'auto'}	{'solver': 'adam', 'hidden_ layer_sizes': (100, 100, 100), 'alpha': 0.01, 'activation': 'relu', 'learning_rate':0.001,0.01}	{'kernel': 'linear', 'C': 100}

Table 3. Finger vein images quality evaluation results.

Images	Average	Contrast	Entropy	GCF	Wang17	HSNR	PSNR	SSIM
Org	128.109	0.232	7.367	2.463	0.071	10.0	1.0	0.1
Gabor	128.528	0.229	7.415	2.455	0.639	90.562	31.501	0.805
CLAHE	127.241	0.273	7.572	2.521	0.708	85.178	19.082	0.788
HFEF	127.001	0.264	7.517	2.509	0.584	89.196	19.655	0.664
Img-Fus	**137.702**	**0.288**	**7.994**	**2.552**	**0.748**	**97.720**	**34.721**	**0.818**
Cont-Fus	**145.812**	**0.292**	**8.220**	**2.579**	**0.763**	**99.198**	**47.137**	**0.956**

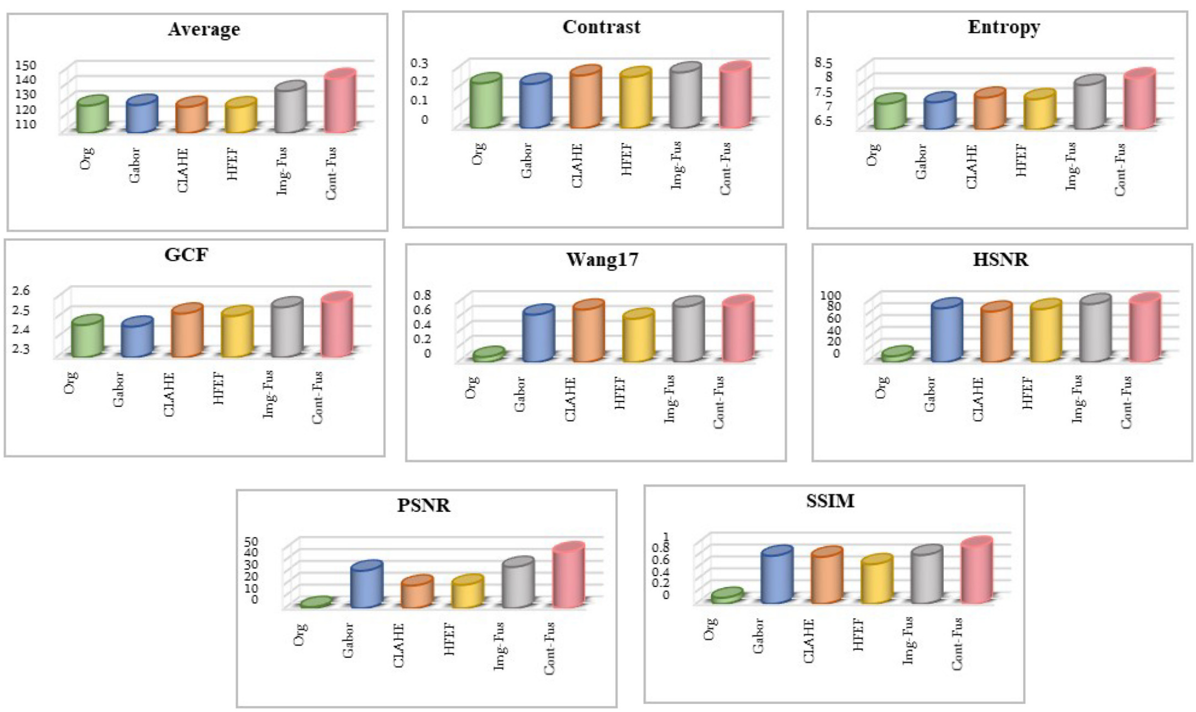

Fig. 5. Show best metrics for finger vein.

that ought to be supplied by experimentation. The performance of ML models depends critically on the selection of ideal hyperparameter set. Table 2 lists several examples of the optimal parameters (best estimator) for the random search model (Hyper Parameter) for ML techniques (MLP, KNN, and SVM), which includes; optimizer used, kernel size, activation, learning rate and hidden layer sizes.

4. Evaluation results

The results of the feature and image quality assessments are shown in this section, along with two models for assessing the authentication system's effectiveness.

4.1. Image quality evaluation

We assessed eight metrics: Contrast, Average, Entropy [44], GCF [45], Wang17 [46], PSNR, HSNR, and SSIM [47] for comparing the quality of improved images with finger-vein datasets that are already available. We assess six images produced by the suggested image enhancement technique in this study. Higher image quality is highlighted in Table 3's results of the image quality evaluation.

In this table, we observe from our experiments, that the results were higher and excellent in both of them (image fusion and contrast image fusion). The results for each high-quality image give a higher performance to the authentication system. Fig. 5 shows a comparison of the six images for the best metrics.

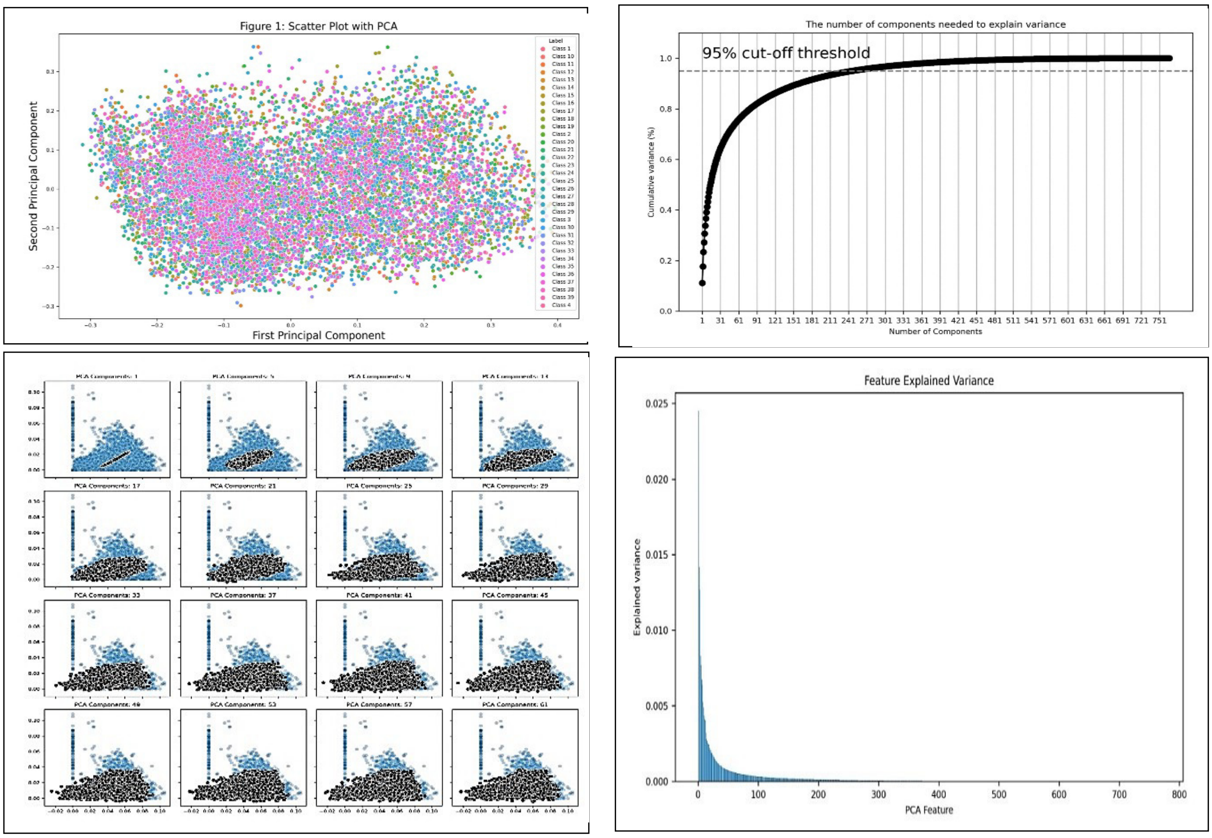

(a)

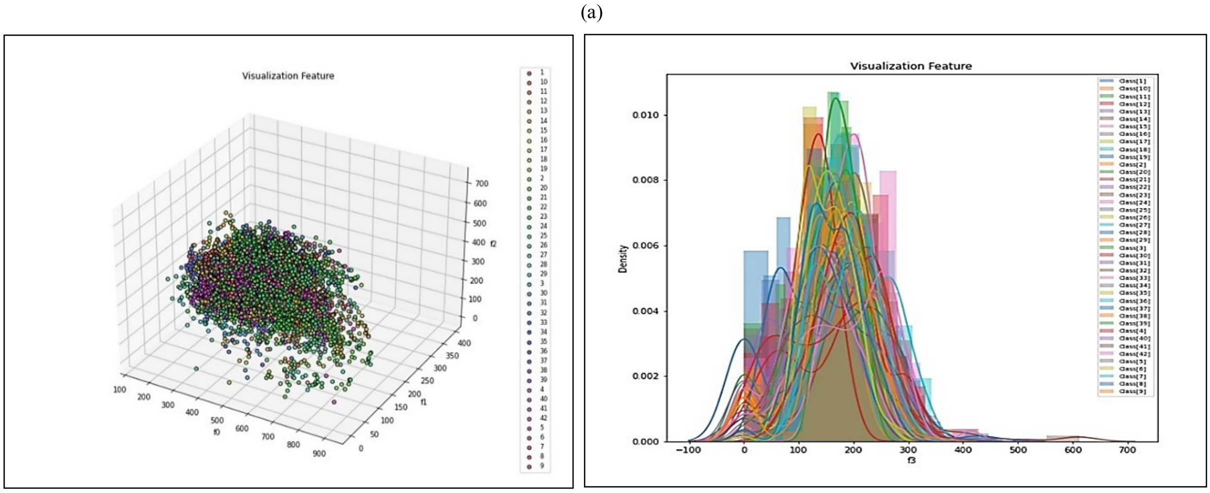

(b)

Fig. 6. Results of PCANet feature extraction method: (a) a scatter plot with PCA, number of components, PCA components, feature explained variance, (b) 2D and 3D plot.

4.2. Evaluation feature fusion

We assessed the suggested system's performance in terms of both authentication and classification modalities. Initially, we assessed the effectiveness of the suggested approach in the absence of feature fusion by utilizing PCANet in conjunction with and without PCA dimensionality reduction on the FVM, FVI, and FVR of each hand separately. Second, we analyzed the proposed method with the feature fusion step. We specifically compared the accuracy achieved through three distinct fusions (Feature Fusion all (Feature Fusion FV-L + Feature Fusion FV-R), Feature Fusion FV-L, and Feature Fusion FV-R. However, we obtained of the feature vectors for each class in datasets as follows:

Table 4. Shows the F1-score for MPML with and without PCA (without preprocessing).

F1-score (%)						
Model	MPML with PCA			MPML without PCA		
Method	KNN	MLP	SVM	KNN	MLP	SVM
Finger Vein (Original Images)						
Fusion all (FV-L + FV-R)	**74.38**	**76.89**	**57.18**	**71.38**	**71.80**	**56.88**
Fusion FV-L	**69.56**	**67.81**	**57**	**68.99**	**64.89**	**55.13**
FV-LI	63.01	57.97	12.10	61.16	57.44	11.32
FV-LM	**58.82**	56.73	37.95	56.78	53.21	36.20
FV-LR	58.20	56.93	11.11	60.47	53.28	10.02
Fusion FV-R	**68.05**	**61.14**	**38.09**	**66.86**	**57.27**	**28.33**
FV-RI	61.05	57.38	32.63	62.09	53.89	30.17
FV-RM	56.82	57.02	31.45	59.73	55.62	29.10
FV-RR	65.20	22.37	30.42	61.77	20.69	37.87

Table 5. Shows the F1-score for HPML with and without PCA (without preprocessing).

F1-score (%)						
Model	MPML with PCA			MPML without PCA		
Method	KNN	MLP	SVM	KNN	MLP	SVM
Finger Vein (Original Images)						
Fusion all (FV-L + FV-R)	**88.72**	**79.14**	**88.82**	**86.34**	**78.26**	**86.44**
Fusion FV-L	**79.30**	**72.84**	**60.74**	**74.67**	**70.89**	**59.89**
FV-LI	82.77	65.50	58.47	81.67	61.80	56.46
FV-LM	87.08	76.59	83.15	84.24	74.30	81.21
FV-LR	61.77	73.03	73.92	60.78	70.47	68.49
Fusion FV-R	**71.79**	**75.79**	**60.92**	**69.70**	**74.30**	**58.34**
FV-RI	67.30	74.21	81.35	64.86	70.71	76.69
FV-RM	83.95	65.31	86.61	81.67	61.78	84.86
FV-RR	73.63	78.52	66.80	70.89	76.13	65.37

Table 6. Shows the F1-score for MPML with and without PCA (with preprocessing).

F1-score (%)						
Model	MPML with PCA			MPML without PCA		
Method	KNN	MLP	SVM	KNN	MLP	SVM
Finger Vein (Enhanced Images)						
Fusion all (FV-L + FV-R)	**95.63**	**97.33**	**99.53**	**94.23**	**94.59**	**98.33**
Fusion FV-L	**95.61**	**96.84**	**99.48**	**92.63**	**90.73**	**98.29**
FV-LI	93	95.51	95.30	92.11	93.74	49.04
FV-LM	93.84	96.21	93.88	86.14	98.30	97.99
FV-LR	94.55	97	93.94	94.84	99.51	34.79
Fusion FV-R	**94.23**	**96.44**	**95.68**	**92.63**	**88.26**	**93.62**
FV-RI	93.84	95.55	99.78	92.11	88.26	99.34
FV-RM	93.51	96.65	99.34	86.14	98.88	99.54
FV-RR	94.55	97.74	99.35	94.84	96.16	96.72

(1) Feature Fusion all: 180, (2) Feature Fusion FV-L: 90, (3) Feature FV-LI: 30, (4) Feature FV-LM:30, (5) Feature FV-LR:30, (6) Feature Fusion FV-R: 90, (7) Feature FV-RI:30, (8) Feature FV-RM:30, (9) Feature FV-RR:30.

Examples of PCANet outputs are shown in Fig. 6. In this figure, we show the filter result from the PCANet layer, some sample outputs after the hashing step, the last output layer of the finger vein, a scatter plot with and without PCA, the number of components needed to explain the variance, the PCA components, the explained variance of the features, and We evaluate the robust features by illustrating 2D and 3D plot visualization features.

4.3. Model evaluation for hyper parameters tuning

For evaluating the efficiency regarding the proposed system by two models: Model Parameter Machine Learning (MPML) and Hyper Parameter Machine Learning (HPML) with and without PCA dimensionality reduction, a set of metrics [48–51] was used (see Eqs. (15) and (18)).

$$Accuracy = \frac{TP + TN}{TP + FN + FP + TN} \tag{15}$$

Table 7. Shows the F1-score for HPML with and without PCA (with preprocessing).

F1-score (%)						
Model	MPML with PCA			MPML without PCA		
Method	KNN	MLP	SVM	KNN	MLP	SVM
Finger Vein (Enhanced Images)						
Fusion all (FV-L + FV-R)	**99.90**	**100**	**100**	**98.68**	**99.68**	**99.93**
Fusion FV-L	**99.06**	**100**	**100**	**98.21**	**99.62**	**99.77**
FV-LI	98.75	100	99.80	98.05	100	99.55
FV-LM	94.73	100	98.25	92.69	98.83	99.77
FV-LR	98.37	100	100	97.37	99.81	100
Fusion FV-R	**98.49**	**100**	**99.78**	**97.53**	**99.57**	**99.83**
FV-RI	97.53	100	100	97.16	99.57	99.93
FV-RM	98.45	100	100	96.87	98.73	100
FV-RR	98.02	100	99.55	97.08	98.45	99.56

Table 8. Compares the image quality evaluation results for the suggested data-sets with several of the existing datasets finger veins.

Datasets	Average	Contrast	Entropy	GCF	Wang17	HSNR
PLUSVein-FV(Proposed)	**12.9551**	**0.262**	**7.5980**	**2.51**	**0.680**	**93.64**
SDUMLA-HMT	0.2799	0.0386	6.6903	0.986	0.165	80.32
HKPU-FID	-	-	-	1.46	0.166	88.13
UTFVP	-	-	-	1.47	0.356	87.15
MMCBNU_6000	-	-	-	1.52	0.121	87.39
FV-USM	0.4467	0.0306	6.7938	0.69	0.136	83.35
PLUSVein-FV3	-	-	-	1.48	0.306	89.78

Fig. 7. Comparison results of HPML for (KNN, MLP, and SVM) methods for original image and enhanced images.

$$Precision = \frac{TP}{TP + FP} \tag{16}$$

$$Recall = \frac{TP}{TP + FN} \tag{17}$$

$$F1\text{-}score = 2 \times \frac{Precision \times Recall}{Precision + Recall} \tag{18}$$

We present the F1-score measure for both models (MPML and HPML) for three methods (KNN, MLP,

Table 9. Comparison of the suggested techniques with some related works

No. of Reference	Use the Dataset	Preprocessing Methods	Feature Extraction Methods	Types of Machine Learning Methods	Matching Results
[15]	collected from 10 individuals by taking 10 images for per finger	-	PCA + LDA	SVM + ANFIS	Accuracy = 98%
[16]	PKU (V2)	CLAHE	GF	SVM	Accuracy = 93.33%
[21]	USM (FV-USM)	Extraction of ROI	PCA	akNCN	Accuracy = 85.64%
[23]	collected from 10 samples per finger and 10 subjects	-	PCA	Integrated BP network, and ANFIS	Accuracy = 97%
[24]	collected using infrared (850nm-940nm) for 600 images	Image Cropping	PCA	BP network	Accuracy = 81%
[28]	SDUMLA-HMT	Binarization, Sobel Filter, Extraction of ROI, and Local Histogram	Combined FAST and FRKP	KNN DA	Accuracy = 55.84%, 92.21%
[29]	FV-USM	-	SRC	KNN	Accuracy = 91.29%
[33]	HKPU, PLUSVein-Contactless finger vein, PMMDB, and UTFVP	Mask R-CNN, CCNet and HRNet using for Segmentation	-	-	Accuracy = 95%, 97%, and 98% for HKPU, 96%,94%, and 95% for PLUSVein-Contactless finger vein, 97%,97%,and 99% for PMMDB, and 95%, 97%, and 99% for UTFVP
Our Proposed	PLUSVein-Contactless finger vein	Proposed new enhanced image methods (Image Fusion) use CLAHE, Gabor Filter, and HFEF	Proposed a new integrated PCA Net deep learning with PCA	Proposed Machine learning models (Model Parameter and Hyper Parameter) apply on KNN, MLP, and SVM methods	F1 score = 99.90% 100% and 100%

and SVM), and the results for the original images before using the proposed image enhancement methods and after applying the image enhancement methods are presented in the Tables 4 and 5 and Tables 6 and 7 for evaluating the performance regarding the authentication system. Training as well as testing sets of the dataset had been split before the system was trained. The test set was then used to evaluate the methods (KNN, MLP, and SVM).

5. Discussion

A review of PLUSVein-Contactless dataset was conducted. The results are displayed in Table 3 after comparing the set of metrics (Contrast, Average, GCF, Entropy, Wang17, PSNR, HSNR, and SSIM) for six images (Original Images, CLAHE Images, Image Images, Contrast Images, and HFEF Images). When we applied the improvement approaches to the original finger vein images, we saw that the metrics increased significantly. We found that for the PLUSVein-Contactless dataset, every metric value for the images processed (contrast and image fusion) by our method takes the maximum value. On the contrary, for the processed images (the HFEF and CLAHE images), PSNR, HSNR, and SSIM take the lowest average value. It is evident that the treated images (Gabor image) have the lowest values for entropy, GCF, and Wang17. We examine several publicly available finger vein data-sets using the same metrics of quality. SDUMLA-HMT [26], HKPU-FID [52], UTFVP [53], MMCBNU6000 [54], FV-USM [22], and PLUSVein-FV-3 [55] are data-sets that are available for finger vein. Table 8 presents the evaluation outcomes. Our suggested dataset produced the best results for a suggested set of metrics when finger veins were taken into account. These findings highlight both good contrast quality and good vein-specific feature quality in images. We choose to concentrate on assessing authentication accuracy because the authentication system's performance is impacted by the evaluation of image quality.

In the following, we performed several performance evaluations of our authentication system, where the highest results were for the enhanced images when we applied PCANet feature level with and without PCA dimensionality reduction for both models: Model Parameter and HyperParameter Model that using the methods (KNN, MLP, and SVM). These models achieved excellent results for the proposed system with decreased time-consuming for matching, where the F1-Score (100%) in MLP and SVM and (99.90%) in KNN with PCA dimensionality reduction, whereas results F1-Score (99.68% and 99.93%) in MLP and SVM methods and (98.68%) in KNN without PCA dimensionality reduction, While the lowest results were for the original image without preprocessing that achieved the lowest results in two models, as the F1-Score reached (88.72% and 86.34%) in KNN, and (79.14% and 78.26%) in MLP, and (88.82% and 86.44%) in SVM methods with and without PCA dimensionality reduction as has been listed in Table 7 and Table 5. The results were satisfactory for both models but we observed several important findings. The Hyper Parameter Model achieved the best results while ranking second for the Model Parameter, due to our choice of the optimal set of parameters and also the result with reduction features based PCA is better than without PCA reduction. Finally, we observed that the hand with the highest outcomes had the fusion of all finger veins (middle, index, and ring fingers) on both hands; nevertheless, the left hand's fusion performed better than the right hand's. To evaluate how well the Hyper Parameter model performed for each of hands' index, middle, and ring finger vein images in both the original and improved versions, as seen in Fig. 7.

A comparison between the proposed system and some related works, as shown in Table 9, highlights its pioneering system. Unlike previous systems, our system's results showed higher authentication accuracy than other previous studies. This system, evaluated against key parameters such as dataset, feature extraction methods, and ML models, clearly demonstrates the system's advantage over existing methods.

6. Conclusion

In the presented study, we suggested a new system to enhance finger vein authentication, this system presents a proposed enhanced method that depends on three methods (CLAHE, GF, and HFEF) to produce high-quality images, implemented on the PLUSVein-Contactless finger vein dataset. The system induces a new feature extraction based on integrated PCANet deep learning and feature-level PCA feature extraction and dimensionality reduction. In addition, it employs the KNN, MLP, and SVM methods for two machine learning models namely: a simple search model (Model Parameter) and a random search model (HyperParameter). Using standard metrics, the hyperparameter model achieved significantly higher results than the model parameter on a dataset of finger vein images captured with high variations in bending, tilts, and rotations of the finger. The use of the proposed system has always allowed to increase in the accuracy of the biometric procedure authentication, concerning the use of the integration of all finger veins or finger vein separately. The system has limitations in improving the matching for higher accuracy and handling similar finger veins. While hyperparameter tuning improves performance, choosing inappropriate parameters can reduce accuracy. This is evident in the middle finger vein of the left hand using the KNN method with and without PCA dimensionality reduction, where results are good but lower than other fingers, further research is needed to address these challenges. To further enhance the robustness of the system, future research will explore more complex feature extraction structures, and different ML approaches, like (random forest, and decision tree) with optimal parameters, and use PLUSVein-Contactless hand VeinRL850nm and RL950nm datasets, we are in the process of completing work on these proposed datasets.

Competing interests

The authors have no competing interests to declare.

Authors' contribution statement

Raniah Ali Mustafa suggested the idea of the manuscript, finding data sets, creating the applied aspect, drawing figures and descriptive tables, writing algorithms, and analyzing and comparing the results.

Tarek Abbes developed the idea of the manuscript, contributed to writing it and developing the methodology, and revised the manuscript.

References

1. N. M. Kamaruddin and B. A. Rosdi, "A new filter generation method in PCANet for finger vein recognition," *IEEE Access*, vol. 7, pp. 132966–132978, 2019. https://doi.org/10.1109/ACCESS.2019.2941555.
2. A. Mathew and P. Amudha, "Enhancing finger vein authentication through deep learning: A comparative study of

U-Net and sequential models," *Journal of Advanced Research in Applied Sciences and Engineering Technology*, vol. 47, no. 1, pp. 230–243, 2024. https://doi.org/10.37934/araset.47.1.230243.
3. H. L. Zayed, H. M. A. Hamid, Y. M. Kamal, and A. H. A. Zekry, "A comprehensive survey on finger vein biometric," *Journal of Advances in Information Technology*, vol. 14, no. 2, pp. 2–8, 2023. https://doi.org/10.12720/jait.14.2.212-223.
4. A. Uhl, C. Busch, S. Marcel, and R. Veldhuis. "Handbook of vascular biometrics", Springer Nature, 2020. https://doi.org/10.1007/978-3-030-27731-4.
5. Y. Bouzouina and L. Hamami, "Multimodal biometric: Iris and face recognition based on feature selection of iris with GA and scores level fusion with SVM," In *2017 2nd International Conference on Bio-engineering for Smart Technologies (BioSMART)*, IEEE, pp. 1–7, 2017. https://doi.org/10.1109/biosmart.2017.8095312.
6. N. Hezil and A. Boukrouche, "Multimodal biometric recognition using human ear and palmprint," *IET Biometrics*, vol. 6, no. 5, pp. 351–359, 2017. https://doi.org/10.1049/iet-bmt.2016.0072.
7. P. S. Chanukya and T. Thivakaran, "Multimodal biometric cryptosystem for human authentication using fingerprint and ear," *Multimedia Tools and Applications*, vol. 79, no. 1, pp. 659–673, 2020. https://doi.org/10.1007/s11042-019-08123-w.
8. B. Ammour, L. Boubchir, T. Bouden, and M. Ramdani, "Face–iris multimodal biometric identification system," *Electronics*, vol. 9, no. 1, p. 85, 2020. https://doi.org/10.3390/electronics9010085.
9. C. Ding and D. Tao, "Robust face recognition via multimodal deep face representation," *IEEE Transactions on Multimedia*, vol. 17, no. 11, pp. 2049–2058, 2015. https://doi.org/10.1109/tmm.2015.2477042.
10. S. Soleymani, A. Torfi, J. Dawson, and N. M. Nasrabadi, "Generalized bilinear deep convolutional neural networks for multimodal biometric identification," In *2018 25th IEEE International Conference on Image Processing (ICIP)*, IEEE, pp. 763–767, 2018. https://doi.org/10.1109/icip.2018.8451532.
11. S. Srinivas and R. V. Babu, "Deep learning in neural networks: An overview," *Computer Science*, 2015. http://dx.doi.org/10.1016/j.neunet.2014.09.003.
12. H. C. Lee, B. J. Kang, E. C. Lee, and K. R. Park, "Finger vein recognition using weighted local binary pattern code based on a support vector machine," *Journal of Zhejiang University SCIENCE C*, vol. 11, no. 7, pp. 514–524, 2010. https://doi.org/10.1631/jzus.c0910550.
13. Y. Yang, J. Li, and Y. Yang, "The research of the fast SVM classifier method," In *2015 12th International Computer Conference on Wavelet Active Media Technology and Information Processing (ICCWAMTIP)*, IEEE, pp. 121–124, 2015. https://doi.org/10.1109/iccwamtip.2015.7493959.
14. A. Romanov, K. Lomotin, and E. Kozlova, "Application of natural language processing algorithms to the task of automatic classification of Russian scientific texts," *Data Science Journal*, vol. 18, pp. 37–37, 2019. https://doi.org/10.5334/dsj-2019-037.
15. J.-D. Wu and C.-T. Liu, "Finger-vein pattern identification using SVM and neural network technique," *Expert Systems with Applications*, vol. 38, no. 11, pp. 14284–14289, 2011. https://doi.org/10.1016/j.eswa.2011.05.086.
16. S. Khellat-Kihel, N. Cardoso, J. Monteiro, and M. Benyettou, "Finger vein recognition using Gabor filter and support vector machine," In *International Image Processing, Applications and Systems Conference*, IEEE, pp. 1–6, 2014. https://doi.org/10.1109/ipas.2014.7043263.
17. S. Bharathi and R. Sudhakar, "Biometric recognition using finger and palm vein images," *Soft Computing*, vol. 23, no. 6, pp. 1843–1855, 2019. https://doi.org/10.1007/s00500-018-3295-6.
18. A. M. Reza, "Realization of the contrast limited adaptive histogram equalization (CLAHE) for real-time image enhancement," *Journal of VLSI Signal Processing Systems for Signal, Image and Video Technology*, vol. 38, pp. 35–44, 2004. https://doi.org/10.1023/b:vlsi.0000028532.53893.82.
19. M. S. Hitam, E. A. Awalludin, W. N. J. H. W. Yussof, and Z. Bachok, "Mixture contrast limited adaptive histogram equalization for underwater image enhancement," In *2013 International Conference on Computer Applications Technology (ICCAT)*, IEEE, pp. 1–5, 2013. https://doi.org/10.1109/iccat.2013.6522017.
20. P. Kalaimathi and V. Ganesan, "Extraction and authentication of biometric finger vein using gradient boosted feature algorithm," In *2016 International Conference on Communication and Signal Processing (ICCSP)*, IEEE, pp. 0723–0726, 2016. https://doi.org/10.1109/iccsp.2016.7754239.
21. B. A. Rosdi, N. Mukahar, and N. T. Han, "Finger vein recognition using principle component analysis and adaptive k-nearest centroid neighbor classifier," *International Journal of Integrated Engineering*, vol. 13, no. 1, pp. 177–187, 2021. https://doi.org/10.30880/ijie.2021.13.01.016.
22. M. S. M. Asaari, S. A. Suandi, and B. A. Rosdi, "Fusion of band limited phase only correlation and width centroid contour distance for finger based biometrics," *Expert Systems with Applications*, vol. 41, no. 7, pp. 3367–3382, 2014. https://doi.org/10.1016/j.eswa.2013.11.033.
23. J.-D. Wu and C.-T. Liu, "Finger-vein pattern identification using principal component analysis and the neural network technique," *Expert Systems with Applications*, vol. 38, no. 5, pp. 5423–5427, 2011. https://doi.org/10.1016/j.eswa.2010.10.013.
24. C. He, Z. Li, L. Chen, and J. Peng, "Identification of finger vein using neural network recognition research based on PCA," In *2017 IEEE 16th International Conference on Cognitive Informatics & Cognitive Computing (ICCI* CC)*, IEEE, pp. 456–460, 2017. https://doi.org/10.1109/icci-cc.2017.8109788.
25. R. Ramaprabha and Dr. V. K. David, "Authentication based on finger vein recognition using neuro-fuzzy technique," *International Journal of Applied Engineering Research*, ISSN 0973-4562, Vol. 10, no. 20, pp. 41508–41512, 2015.
26. Y. Yin, L. Liu, and X. Sun, "SDUMLA-HMT: A multimodal biometric database," In *Biometric Recognition: 6th Chinese Conference, CCBR* 2011, Beijing, China, December 3–4, 2011. Proceedings 6, pp. 260–268, 2011. Springer. https://doi.org/10.1007/978-3-642-25449-9_33.
27. Q. E. Wen, N. M. Kamaruddin, and B. A. Rosdi, "Raspberry Pi-based finger vein recognition system using PCANet," In *Journal of Physics: Conference Series*, IOP Publishing, vol. 1529, no. 2, p. 022068, 2020. https://doi.org/10.1088/1742-6596/1529/2/022068.
28. R. Khanam, R. Khan, and R. Ranjan, "Analysis of finger vein feature extraction and recognition using DA and KNN methods," In *2019 Amity International Conference on Artificial Intelligence (AICAI)*, IEEE, pp. 477–483, 2019. https://doi.org/10.1109/aicai.2019.8701253.
29. S. Shazeeda and B. Rosdi, "Finger vein identification based on the fusion of nearest neighbor and sparse representation based classifiers," *Indian J Sci Technol*, vol. 9, no. 48, pp. 1–7, 2016. https://doi.org/10.17485/ijst/2016/v9i48/109315.

30. S. J. Xie, S. Yoon, J. Yang, Y. Lu, D. S. Park, and B. Zhou, "Feature component-based extreme learning machines for finger vein recognition," *Cognitive Computation*, vol. 6, pp. 446–461, 2014. https://doi.org/10.1007/s12559-014-9254-3.
31. P. Padmapriya, J. Saminathan, I. L. Priya, and M. Dayanidhy, "Deep learning-based biometric finger vein authentication system for enhanced security," *International Journal for Multidisciplinary Research (IJFMR)*, vol. 6, Issue 5, 2024. https://doi.org/10.36948/ijfmr.2024.v06i05.27652.
32. A. Rehman, M. Harouni, M. Omidiravesh, S. M. Fati1, and S. A. Bahaj, "Finger vein authentication based on wavelet scattering networks," *Computers, Materials & Continua*, vol. 27, no. 2, 2022. https://doi.org/10.32604/cmc.2022.016410.
33. B. Prommegger, D. Sollinger, G. Wimmer, and A. Uhl, "CNN based finger region segmentation for finger vein recognition," In *2022 International Workshop on Biometrics and Forensics (IWBF)*, IEEE, pp. 1–6, 2022. https://doi.org/10.1109/iwbf55382.2022.9794514.
34. B. Prommegger, G. Wimmer, and A. Uhl, "Cross sensor finger vein recognition," In *2022 International Conference of the Biometrics Special Interest Group (BIOSIG)*, IEEE, pp. 1–5, 2022. https://doi.org/10.1109/BIOSIG55365.2022.9896962.
35. T.-H. Chan, K. Jia, S. Gao, J. Lu, Z. Zeng, and Y. Ma, "PCANet: A simple deep learning baseline for image classification?" *IEEE Transactions on Image Processing*, vol. 24, no. 12, pp. 5017–5032, 2015. https://doi.org/10.1109/tip.2015.2475625.
36. W. Xinshao and C. Cheng, "Weed seeds classification based on PCANet deep learning baseline," In *2015 Asia-Pacific Signal and Information Processing Association Annual Summit and Conference (APSIPA)*, IEEE, pp. 408–415, 2015. https://doi.org/10.1109/apsipa.2015.7415304.
37. J. Zhao, H. Tian, W. Xu, and X. Li, "A new approach to hand vein image enhancement," In *2009 Second International Conference on Intelligent Computation Technology and Automation*, IEEE, vol. 1, pp. 499–501, 2009. https://doi.org/10.1109/ICICTA.2009.127.
38. M. B. A. Haghighat, A. Aghagolzadeh, and H. Seyedarabi, "Multi-focus image fusion for visual sensor networks in DCT domain," *Computers & Electrical Engineering*, vol. 37, no. 5, pp. 789–797, 2011. https://doi.org/10.1016/j.compeleceng.2011.04.016.
39. A. A. Abbood, M. S. H. Al-Tamimi, S. U. Peters, G. Sulong, J. B. Skudai, and A. A. Abbood, "New Combined Technique for Fingerprint Image Enhancement," *Modern Applied Science*, vol. 11, no. 1, pp. 222–234, 2016. https://doi.org/10.5539/mas.v11n1p222.
40. J. Zheng and C. Rakovski, "On the application of principal component analysis to classification problems," 2021. https://doi.org/10.5334/dsj-2021-026.
41. J.-D. Wu and C.-T. Liu, "Finger-vein pattern identification using principal component analysis and the neural network technique," *Expert Systems with Applications*, vol. 38, no. 5, pp. 5423–5427, 2011. https://doi.org/10.1016/j.eswa.2010.10.013.
42. J. Kurek *et al.*, "Improved drill state recognition during milling process using artificial intelligence," *Sensors*, vol. 23, no. 1, p. 448, 2023. https://doi.org/10.3390/s23010448.
43. S. Raghu and N. Sriraam, "Optimal configuration of multilayer perceptron neural network classifier for recognition of intracranial epileptic seizures," *Expert Systems with Applications*, vol. 89, pp. 205–221, 2017. https://doi.org/10.1016/j.eswa.2017.07.029.
44. S. Shazeeda and B. A. Rosdi, "Nearest centroid neighbor based sparse representation classification for finger vein recognition," *IEEE Access*, vol. 7, pp. 5874–5885, 2018. https://doi.org/10.1109/ACCESS.2018.2889506.
45. K. Matkovic, L. Neumann, A. Neumann, T. Psik, and W. Purgathofer, "Global contrast factor-a new approach to image contrast," In *CAe*, 2005, pp. 159–167.
46. C. Wang, X. Zeng, X. Sun, W. Dong, and Z. Zhu, "Quality assessment on near infrared palm vein image," In *2017 32nd Youth Academic Annual Conference of Chinese Association of Automation (YAC)*, IEEE, pp. 1127–1130, 2017. https://doi.org/10.1109/yac.2017.7967580.
47. H. Ma, F. P. Cui, and P. Oluwatoyin P, "A non-contact finger vein image quality assessment method," *Applied Mechanics and Materials*, vol. 239, pp. 986–989, 2013. https://doi.org/10.4028/www.scientific.net/AMM.239-240.986.
48. Z. Hashim, H. Mohsin, and A. Alkhayyat, "Offline handwritten signature identification based on hybrid features and proposed deep model," *Iraqi Journal for Computer Science and Mathematics,* vol. 5, no. 1, p. 220–236, 2024. https://doi.org/10.52866/ijcsm.2024.05.01.016.
49. A. Saad, M. M. A. Zabidi, I. S. Kamil, and U. U. Sheikh, "A novel deep learning approach for classification of bird sound using mel frequency cepstral coefficients," *Iraqi Journal for Computer Science and Mathematics,* vol. 5, no. 3, pp. 660–670, 2024. https://doi.org/10.52866/ijcsm.2024.05.03.040.
50. M. J. Nabet and L. E. George, "Phishing attacks detection by using artificial neural networks," *Iraqi Journal for Computer Science and Mathematics,* vol. 4, no. 3, pp. 159–166, 2023. https://doi.org/10.52866/ijcsm.2023.02.03.013.
51. H. A. Salman and A. Kalakech, "Image enhancement using convolution neural networks," *Babylonian Journal of Machine Learning,* vol. 2024, pp. 30–47, 2024. https://doi.org/10.58496/BJML/2024/003.
52. A. Kumar and Y. Zhou, "Human identification using finger images," *IEEE Transactions on Image Processing*, vol. 21, no. 4, pp. 2228–2244, 2011. https://doi.org/10.1109/TIP.2011.2171697.
53. B. T. Ton and R. N. Veldhuis, "A high quality finger vascular pattern dataset collected using a custom designed capturing device," In *2013 International Conference on Biometrics (ICB)*, IEEE, pp. 1–5, 2013. https://doi.org/10.1109/icb.2013.6612966.
54. Y. Lu, S. J. Xie, S. Yoon, Z. Wang, and D. S. Park, "An available database for the research of finger vein recognition," In *2013 6th International Congress on Image and Signal Processing (CISP)*, IEEE, vol. 1, pp. 410–415, 2013. https://doi.org/10.1109/cisp.2013.6744030.
55. C. Kauba, B. Prommegger, and A. Uhl, "Focussing the beam-a new laser illumination based data set providing insights to finger-vein recognition," In *2018 IEEE 9th International Conference on Biometrics Theory, Applications and Systems (BTAS)*, IEEE, pp. 1–9, 2018. https://doi.org/10.1109/btas.2018.8698588.